JOC The Journal of Organic Chemistry

JOCSynopsis

pubs.acs.org/joc

Using Electron Paramagnetic Resonance Spectroscopy To Facilitate Problem Solving in Pharmaceutical Research and Development

Ian Mangion,* Yizhou Liu,* Mikhail Reibarkh, R. Thomas Williamson, and Christopher J. Welch

Department of Process & Analytical Chemistry, Merck Research Laboratories, Rahway, New Jersey 07065, United States

ABSTRACT: As new chemical methodologies driven by single-electron chemistry emerge, process and analytical chemists must develop approaches to rapidly solve problems in this nontraditional arena. Electron paramagnetic resonance spectroscopy has been long known as a preferred technique for the study of paramagnetic species. However, it is only recently finding application in contemporary pharmaceutical development, both to study reactions and to track the presence of undesired impurities. Several case studies are presented here to illustrate its utility in modern pharmaceutical development efforts.

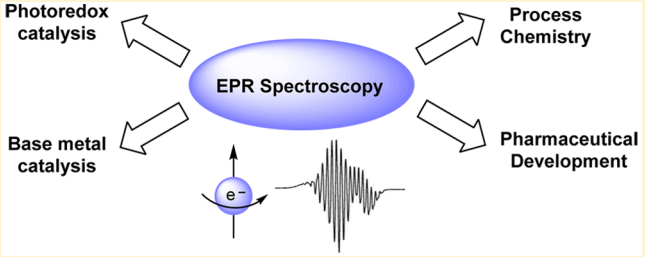

INTRODUCTION

Two of the fundamental principles of synthetic chemistry processes are that they be predictable and controllable at both small and large scale. Thus, pharmaceutical chemistry development historically centered on well-understood reactions where net oxidation level either does not change or undergoes change in predictable two-electron increments (e.g., anion or cation chemistry, two electron oxidations and reductions, etc.). In other fields, radical-based chemistry has been well studied for decades as a keystone technology for 20th century polymer and bulk chemicals manufacturing. However, harnessing the turbulent reactivity of organic radicals to achieve broadly useful regio- and stereoselective reactions in pharmaceutical manufacturing has been challenging, with a few notable exceptions.[1]

Recent years have seen a marked increase in the understanding of new chemical reactions involving unpaired electrons. These developments offer exciting opportunities for rapid, efficient, controllable, and economical bond formation. Indeed, the renaissance of visible light photoredox catalysis has placed the chemistry of organic radicals at the forefront of organic synthesis.[2,3] Similarly, electrochemistry, once largely confined to analysis or industrial production of bulk materials, is now being fervently explored as a platform for new synthetic reactions involving radical intermediates.[4] Recent interest in catalysis using earth-abundant "base metals" such as cobalt, iron, and nickel has ballooned,[5] driven both by sustainability considerations[6] and the potential for orthogonal or even superior performance relative to conventional precious metal catalysts. While not radicals per se, these first-row transition metals can often exist in a paramagnetic state and can participate in single-electron redox chemistry more readily than noble metals such as palladium.[7]

Efficient process chemistry development requires extremely close collaboration between synthetic and analytical chemists to solve emerging problems and enable mechanistic understanding. In addition to building tools to address the problems of today, process and analytical chemists must create techniques that provide rapid solutions to the problems of tomorrow. One such example is EPR spectroscopy, a venerable technique for studying species with unpaired electrons.[8] EPR has long been used in the characterization of organic radicals, organometallic complexes, protein structure and dynamics, polymerization chemistry, and radical degradation processes, among other uses.[9] However, the historical use of EPR in pharmaceutical development has been limited, perhaps reflecting the aforementioned paucity of applications of single electron chemistry in the field.[10,11] We herein report an investigation into the application of EPR spectroscopy for analyzing paramagnetic species in support of pharmaceutical development.

While some description of the EPR technique is included in most graduate curricula, most chemists will have had limited opportunities to apply it in practice, so a brief tutorial may be justified. The principles of operation for EPR are reminiscent of those for NMR spectroscopy; however, in EPR spectroscopy, it is the spins of electrons that are excited instead of the spins of atomic nuclei (Figure 1).

While pulsed EPR has gained popularity since the 1990s, the traditional continuous wave (CW) EPR is still preferred in many EPR laboratories. In the CW setup, the sample is irradiated with microwave radiation at a fixed frequency (e.g., ∼9 GHz for X-band or ∼35 GHz for Q-band), while the magnetic field is scanned in search of the resonance condition. When the energy gap between the two electron spin states (which is proportional to the magnetic field strength) matches the energy of the incident photon, an EPR signal emerges due to photon absorption. The resonance condition is described by the following equation

$$h\nu = g\beta B \quad (1)$$

Special Issue: Photocatalysis

Received: April 25, 2016
Published: June 20, 2016

DOI: 10.1021/acs.joc.6b00937
J. Org. Chem. 2016, 81, 6937−6944

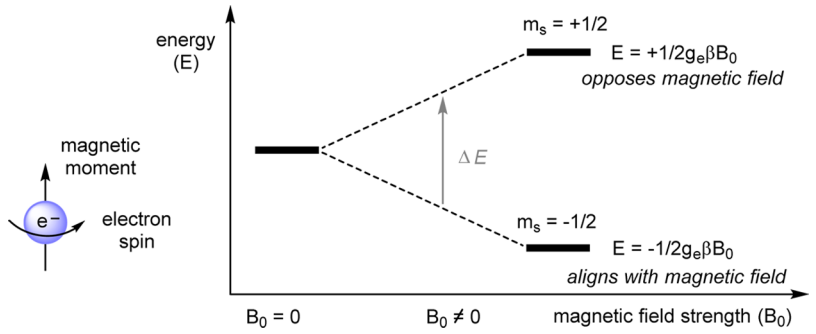

Figure 1. Splitting of the electron spin energy level induced by a magnetic field.

where h is Planck's constant, ν is the microwave frequency, β is Bohr magneton, B is the magnetic field strength, and g is a dimensionless factor that depends on the environment in which the unpaired electron resides. For a free electron, the g factor, g_e, is found to be 2.0023. The g factor is the most easily measurable EPR parameter, dictating at what field strength an EPR signal occurs during a CW experiment.

In addition to the field ramp, a sinusoidal magnetic field modulation is introduced that frequency labels the EPR signal for detection, while background noise and electrical interference are not responsive to this modulating field and thereby can be suppressed by a high-pass filter. This mode of detection, commonly referred to as phase sensitivity detection, gives rise to the well-known CW EPR line-shape that appears as the first derivative of an absorption signal over the magnetic field (Figure 2).

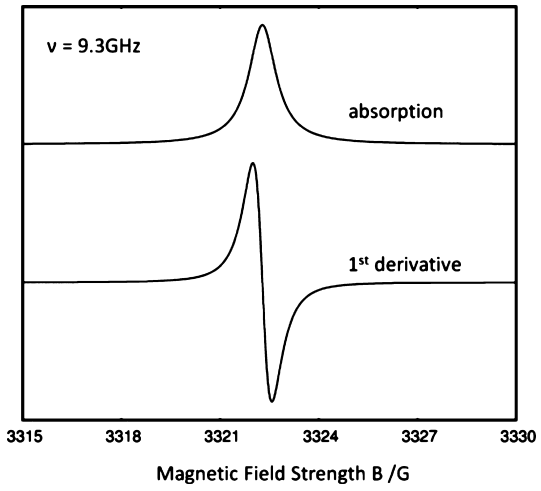

Figure 2. Simulated absorption signal and its first derivative using a g-factor of 2 and line width of 1 G.

EPR spectroscopy detects only those compounds bearing unpaired electrons such as paramagnetic transition metals or organic radicals. Paired electrons necessarily have antiparallel magnetic moments based on Pauli's exclusion principle and, therefore, only form the EPR-silent singlet state. Most solvents do not give rise to EPR signals, allowing detection and structural analysis of paramagnetic compounds in solution. Moreover, EPR spectroscopy is approximately 1000 times more sensitive than NMR, enabling detection of small, transient populations of compounds containing unpaired electrons.

The phenomena of spin-orbit interaction and hyperfine coupling are highly useful for chemical analysis. When an electron is bound to an atom the g factor deviates from g_e in a manner that depends on the spin-orbit interaction, the underlying physics of which is analogous to that of chemical shielding in NMR. In an EPR experiment, the nucleus produces a second magnetic field that shifts the resonance frequency away from that of a free electron. In organic radicals, the spin-orbit interaction is very weak, and therefore, the g factors are very close to g_e. However, in heavier elements such as metals, the g factors can be significantly different from g_e. Thus, by measuring the g factor one can quickly determine whether the unpaired electron resides on an organic ligand or a metal atom. For a metal-centered radical, it is even possible to determine the metal identity and oxidation state, particularly with further information from hyperfine coupling.

Hyperfine coupling arises from an interaction between an electron spin and a nuclear spin and is analogous to J coupling observed in NMR. Unlike the spin-orbit interaction that shifts the resonance line position, the hyperfine coupling splits the EPR signal into multiplets. If an electron spin is simultaneously coupled to N equivalent nuclei of spin S, its EPR signal will have 2NS+1 lines with intensities governed by a bi/multinomial distribution (Figure 3).

By analyzing the multiplet structure of an EPR signal, one can determine the identities and abundance of neighboring nuclear spins. However, this practice becomes challenging with extensive

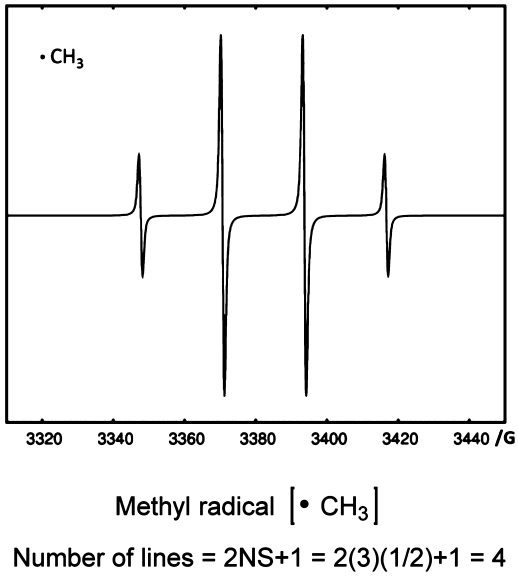

Figure 3. Hyperfine coupling exemplified by the simulated EPR spectrum of the methyl radical.

DOI: 10.1021/acs.joc.6b00937
J. Org. Chem. 2016, 81, 6937−6944

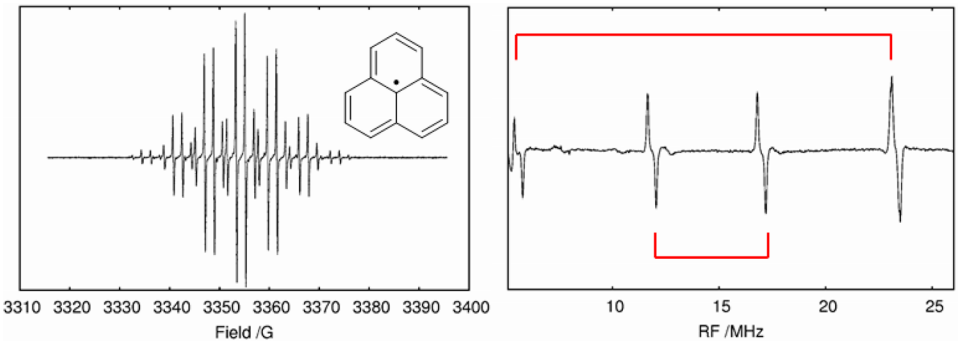

Figure 4. Example of CW-ENDOR used to simplify the analysis of the perinaphthenyl radical. Left, EPR spectrum taken at 298 K with 0.2 mW microwave power. Right, ENDOR spectrum with 5.024 mW microwave power and 3.77 W radiowave attenuation. Pairs of resonances split due to hyperfine couplings are connected by red lines.

coupling. Electron nuclear double resonance (ENDOR) spectroscopy facilitates analysis of complicated hyperfine couplings. In a CW-ENDOR experiment, the magnetic field is fixed to the strongest component in the EPR multiplet rather than being swept as in CW-EPR. Under this condition, that particular EPR transition gets saturated by the strong microwave irradiation. Due to electron−nuclear coupling, the NMR transitions are hyperpolarized as the EPR transition is saturated. Simultaneous irradiation of the sample with a radio frequency sweep identifies those frequencies that saturate the NMR transitions. As NMR transitions are saturated, the EPR transition is repolarized and absorbs energy from the irradiating microwave, thereby producing an ENDOR signal. ENDOR spectroscopy allows one to study nuclear spin transitions but using the much larger electron transition energy for detection. The ENDOR spectrum is virtually an NMR spectrum subject to electron hyperfine splitting. Since each nucleus is only coupled to a single electron spin, the ENDOR spectrum simply contains a pair of doublets for each nonequivalent group of nuclei.

An example of this technique is shown in Figure 4, in which the EPR spectrum of the perinaphthenyl radical produces 28 lines, rendering structural interpretation very challenging. By applying ENDOR spectroscopy, the spectrum is reduced to four lines corresponding to two sets of nonequivalent protons. One drawback of ENDOR is that information regarding the number of atoms that are hyperfine coupled is lost because the signal intensity does not faithfully represent the number of coupled atoms. However, this information can be obtained from the EPR spectrum using the hyperfine coupling constants available from ENDOR.

QUANTITATION AND PRACTICAL LIMITS OF DETECTION

To assess the potential utility of EPR spectroscopy for emergent problems in pharmaceutical research, we acquired a 9.3 GHz X-band EPR instrument and evaluated its use in a series of studies. As a first study, we evaluated the performance of quantitative EPR (qEPR)[12] in low-level radical counting using TEMPO as the model compound. This study also has practical significance as it provides a potentially useful approach for exploring the downstream rejection of this reagent from pharmaceutical processes, necessary because TEMPO is a suspected genotoxic impurity.[13] EPR spectra were collected for 8 TEMPO samples spanning a concentration range of 2−250 μM, and then double-integration and spin counting were carried out.[14] Appropriate signal averaging was applied to samples of various concentrations, with experimental time ranging from 100 s for the most concentrated samples, up to 3 h for the most dilute sample. As shown in Figure 5, good linearity (R = 0.999) was observed between predetermined concentrations and concentrations from qEPR, demonstrating excellent relative spin quantification.[15] The line-fitting slope was determined to be 1.6 instead of 1, indicating a 38% systematic overestimation from spin counting. This discrepancy may arise as the spin counting formula assumes knowledge of certain parameters that may not be accurately known or measured, such as the resonator's Q value and the active sample volume inside the resonator. For applications that require absolute quantification, normalizing with a standard sample can be expected to provide excellent accuracy in light of the good linearity across a significant concentration range as shown in this study. It is also worth pointing out that for quantification of very low level of radicals dissolved in solvents of large electrical dipoles, including DMSO, a flat cell is preferred over the capillary tube used in this study, as the former allows for a much larger sample volume.

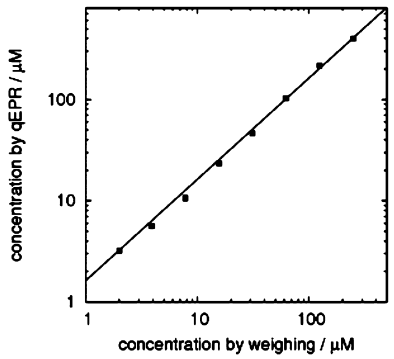

Figure 5. EPR spectrum of TEMPO and plot of EPR signal intensity vs actual concentration.

Interestingly, at low concentrations of TEMPO, it was possible to observe an interfering signal arising from the glass comprising the capillary tubes used in this study (Figure 6). Although this problem can be circumvented by the use of quartz tubes, we highlight this point to draw attention to the sensitivity of the EPR technique.

APPLICATIONS IN PHOTOREDOX CATALYSIS

We next turned our attention to the study of the production of organic free radicals from exposure to light. Visible light photoredox catalysis is becoming more prevalent in organic

DOI: 10.1021/acs.joc.6b00937
J. Org. Chem. 2016, 81, 6937−6944

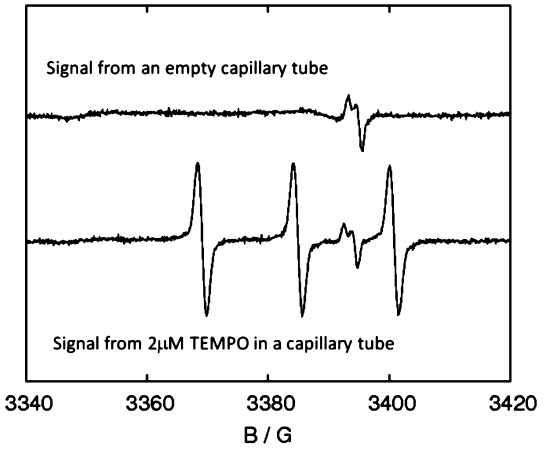

Figure 6. EPR spectrum of TEMPO at 2 μM and signal interference from a borosilicate glass capillary tube.

synthesis, and it is also being incorporated into flow and pharmaceutical processes.[16] As such, there is a great need to understand the mechanisms and kinetics driving these processes to ensure optimal and robust chemistry. Indeed, EPR is already being used with increasing frequency as a tool to refine mechanistic hypotheses for photoredox catalysis.[17] As the diversity of photoredox catalysts grows to encompass organic dyes[18] and transition metals, EPR may afford new possibilities for understanding the reactivity and electronic structure of catalytic intermediates. With accessories for in situ photoexcitation within the EPR probe now commercially available, a broad scope of experiments are accessible to EPR users. For example, Figure 7 shows the EPR spectrum of Fukuzumi's acridnium ion (**1**) with (red) and without (blue) UV irradiation, clearly showing the dependency of the observed excited state on photochemical irradiation.[19]

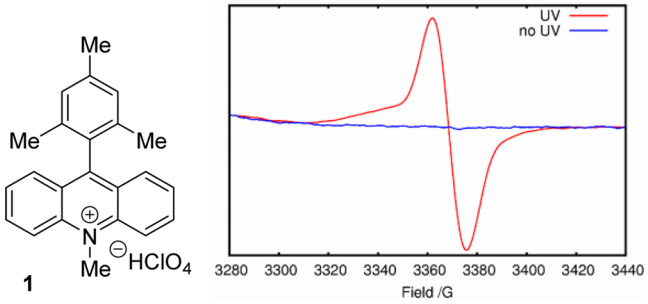

Figure 7. EPR spectrum of acridinium ion **1** upon UV irradiation.

As part of an effort to discover more powerful photoorganic oxidants and reductants, we profiled a series of electronically modified acridinium catalyst architectures.[14] Understanding the reactivity of photocatalysts necessarily focuses on the excited state, as desired reactivity follows from this state. An ideal photocatalyst will need both an excited state with sufficiently high energy and long lifetime to engage in the desired electron transfer process. By modifying the electron density of the acridinium, we hoped to perturb the lifetime of the corresponding excited states, tracking the kinetics of excited state decay for each compound after UV irradiation in PhCN at 223 K.[20,21] As seen in Figure 8, the rate of decay was notably different across a range of acridiniums, with all variants displaying reduced excited state lifetimes relative to **1**. Recent studies have shown such electronic variants to have greater reactivity in a series of photoredox reactions,[22] highlighting the potential value of EPR in new catalyst design and the study of reaction mechanism.

UTILITY OF EPR IN STRUCTURAL ANALYSIS OF BASE METAL COMPLEXES

Interest in earth abundant metals has grown as more economical and sustainable alternatives to precious metal catalysts. In particular, first-row transition metals are being actively examined in a variety of transformations including asymmetric catalysis. First row transition metals often access a broader range of oxidation states than precious metals, and can more readily undergo single electron redox processes. As they do so, they can manifest as paramagnetic species that give rise to EPR spectra, but may be poorly suited to NMR analysis.[23] As the field of transition metal catalysis begins to tilt further toward sustainable base metal catalysis, the scope of possible transformations will grow and EPR will become a standard tool in the mechanistic analysis of these reactions.[24]

Studies into the reactivity of base metal porphyrin complexes led us to consider the EPR spectra for Cu(II) and VO(IV) tetraphenylporphyrin (TPP).[14] Such complexes have been studied in great detail spectroscopically,[25] yet EPR is uniquely suited for the analysis of their electronic structures, and the results exemplify some important features of EPR spectra of metal complexes. As seen in Figure 9, Cu(II) TPP (**6**) displays 4 major peaks consistent with hyperfine interactions with the

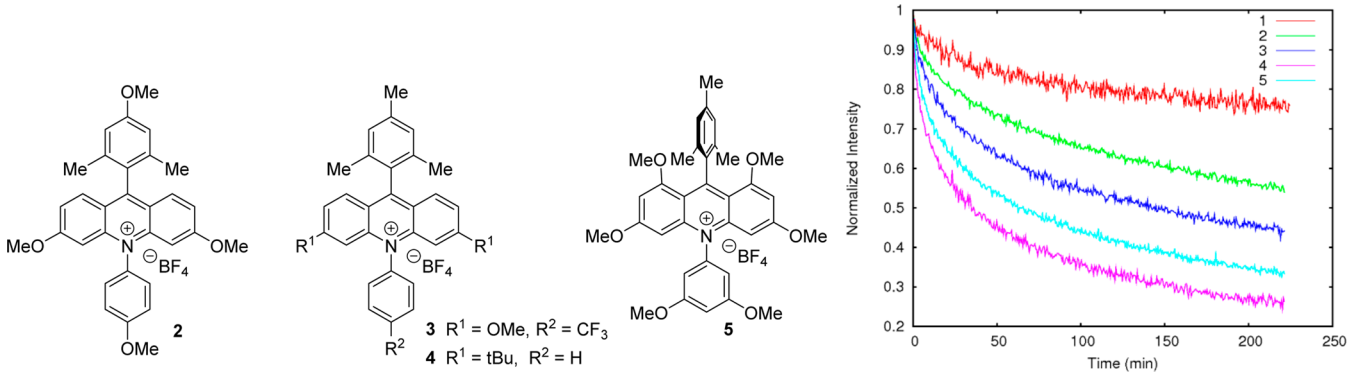

Figure 8. EPR time-course experiments for a series of electronically differentiated acridinium ions. Data were collected at 223 K with acridinium catalysts at 20 mg/mL in PhCN.

DOI: 10.1021/acs.joc.6b00937
J. Org. Chem. 2016, 81, 6937−6944

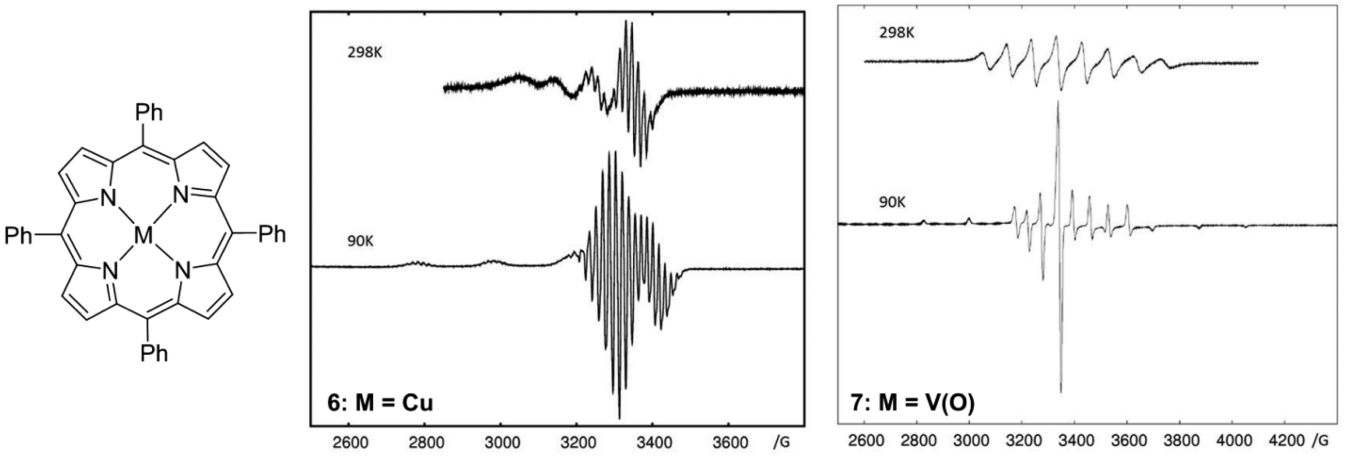

Figure 9. EPR spectra of two related organometallic porphyrin complexes further demonstrating principles of hyperfine couplings.[26]

nuclear spin of Cu (3/2). These four peaks vary in intensity due to differential electron−nuclear interactions, a phenomenon frequently seen in metals. The fine splitting at high fields results from hyperfine coupling to the 4 ^{14}N (spin 1) atoms from the ligand. Freezing the toluene solution at 90 K gives rise to the solid-state spectrum of this sample, characterized by a larger signal spread due to *g*-anisotropy and rich line splittings from hyperfine couplings to nitrogen.

As compared to a solution spectrum, a solid spectrum spans a larger field width as the **g**-tensor is no longer averaged by molecular rotation and has different line structures. These differences are better illustrated by the VO(IV) TPP (**7**) spectra. The major isotope ^{51}V (spin 7/2) leads to 8 peaks at 298 K as expected. A total of 16 peaks are expected in the solid-state spectrum, while only 13 of them are distinct due to overlaps. The difference in line structure, most evident from the weak peaks at low and high ends of the solid spectrum, is more easily appreciated if one considers that the solid spectrum is the first derivative of a broad powder pattern convoluted with both g-anisotropy and hyperfine interactions. A striking difference between Cu(II) and VO(IV) is that hyperfine coupling to nitrogen is not observed for the latter. These results point to important differences in orbital overlap between the two metals and the ligand framework.

SPIN TRAPS AND ANALYSIS OF TRANSIENT SPECIES

Some radical-mediated processes are not easily observed by EPR, featuring radical intermediates too short-lived to observe even at 2−4 K. However, a variety of commercially available "spin traps" can be used to provide EPR evidence of the formation of a radical species.[27] As illustrated in Figure 10, when a transient radical species encounters a spin trap such as DMPO, a more stable nitroxide radical is formed. This stability allows the accumulation of a sufficient concentration of the spin adduct for indirect EPR assessment of the presence of the radical as well as some limited structural analysis.[28] Spin trapping is now a broadly applied technique, with numerous applications in the study of chemical and biological systems.[29]

A recent investigation in our laboratory highlights the potential value of such an approach in the pharmaceutical context. When faced with a puzzling oxidative degradation of a formulated drug product that manifested in some batches, but not others, suspicions arose about the possibility of contamination with metals, trace oxidants in solvents or equipment, or a variety of other unknown factors. Analytical chemistry investigations were inconclusive, only serving to make the process team fear any and all potential culprits, without clearly defining the actual bad actor(s). In this instance, the use of EPR spectroscopy helped to shed light on the situation, bringing the problem under control. In analogy to a technique developed to understand the oxidation of beer,[30,31] the α-phenyl-*N*-*tert*-butyl nitrone (PBN) spin trap was added to dissolved drug product samples (both controls and those undergoing oxidative degradation), and the resulting mixtures evaluated in thermal aging time-course experiments.[14] A representative result of this spin-trap EPR time-course study is illustrated by Figure 11.

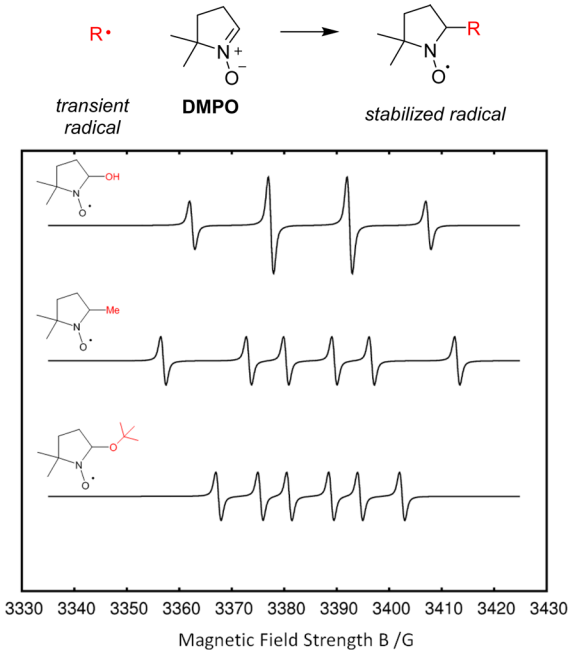

Figure 10. Concept of spin traps, with results exemplified from simulated EPR spectra for three different adducts.

A few features of interest quickly became clear: first, in the presence of the dissolved drug product the spin trap is being consumed at a rate significantly greater than background reactivity of the spin trap in a control experiment in which no drug product is added. Second, no EPR signals are observed in the absence of PBN, indicating only transient radicals are

DOI: 10.1021/acs.joc.6b00937
J. Org. Chem. 2016, 81, 6937−6944

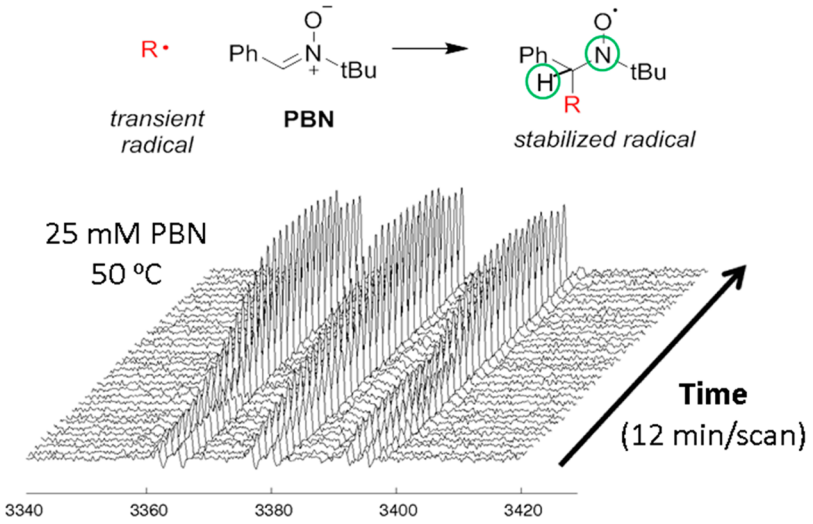

Figure 11. Time course study depicting accumulation of radical spin-trap adducts over time on aging with drug product samples.

produced. Third, the rate of spin-trap consumption varies depending on the batch of drug product added and yet correlated directly with their known long-term stability. Fourth, by conducting the experiments at elevated temperature it was possible to complete individual runs within a day, allowing rapid risk assessment for degradation that would otherwise take months to manifest.

Curiously, multiple species were present during the study, including a short-lived species that diminished within 1 h and a more persistent species that accumulated slowly and eventually reached a plateau. The hyperfine couplings[32] are indicative of peroxyl and hydroxyl radical adducts based on analogy to the literature, although it is challenging to make definitive structural assignments using only the spin-trap data. Nevertheless, this insight led the team to investigate the presence of radical initiators and propagators that could enable production of peroxyl radical species. Further EPR experiments (Figure 12)

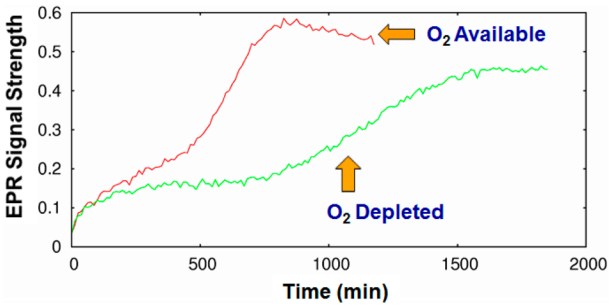

Figure 12. Kinetic dependence of spin-trap consumption on availability of atmospheric oxygen: experiments conducted open to air or in a flame-sealed tube.

conducted in the presence or absence of atmospheric oxygen indeed revealed a kinetic dependence on available oxygen, consistent with traditional mechanistic processes in which radical initiators convert oxygen into radical peroxyl species. The direct involvement of O_2 in radical generation, in turn, led the team to consider protection from air as a simple engineering solution to enhance the stability of the drug product.

This approach clearly illustrates the value of EPR for shedding light on complex situations involving radicals that are otherwise difficult to analyze using conventional techniques. Furthermore, we believe this experimental approach has the potential to be applied more broadly in the context of predicting oxidative stability of pharmaceuticals, either in their pure form or in formulated matrices.

CONCLUSION

In this study, we have presented a diverse array of problems in pharmaceutical research and development that can be probed with EPR spectroscopy. As the use of new 21st century chemistries involving radicals, base metals and other unpaired electron species continue to proliferate, we can look forward to the emergence of EPR from a niche or specialist technique to a mainstay platform for pharmaceutical chemistry analysis.

AUTHOR INFORMATION

Corresponding Authors

*E-mail: ian_mangion@merck.com.
*E-mail: yizhou.liu@merck.com.

Notes

The authors declare no competing financial interest.

Biographies

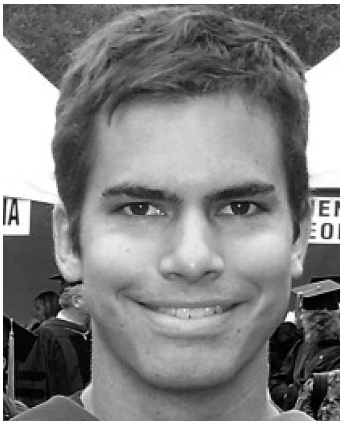

Ian Mangion obtained his Ph.D. studying organic synthesis in the laboratories of David W. C. MacMillan and has been working at Merck in both process and analytical chemistry for the last nine years. He is currently interested in the application of new and emerging analytical tools to the understanding of pharmaceutical processes.

DOI: 10.1021/acs.joc.6b00937
J. Org. Chem. 2016, 81, 6937−6944

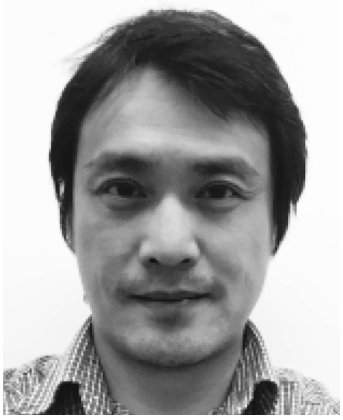

Yizhou Liu obtained his Ph.D. from the Biophysics program at the University of Virginia and did postdoctoral training at the Complex Carbohydrate Research Center at the University of Georgia and the Structural Biology program at Sloan Kettering Institute. His research interests include spectroscopic method development related to NMR and EPR and their applications in chemistry and biology.

Mikhail Reibarkh received his Ph.D. in Biophysics in 2000 from the Moscow Institute of Physics and Technology in Moscow, Russia, followed by postdoctoral fellowships at the University of Michigan and at Harvard Medical School. After working for 2 years at Varian, Inc., he joined the NMR Structure Elucidation Group at Merck in 2009, where his research has focused on developing new NMR methodologies for molecular structure elucidation and utilizing NMR and EPR spectroscopy for physicochemical characterization of small molecules and biomolecules.

R. Thomas Williamson received his Ph.D. from Oregon State University and joined Merck in 2011. Thomas serves as the Director of the NMR Structure Elucidation Group, where he supervises the small molecule NMR group and their support of projects across Merck. Thomas is interested in the elucidation of structures and stereochemistry of complex molecules by NMR and the design of pulse sequences to help achieve this.

Christopher J. Welch has a longstanding interest in identifying and implementing new enabling technologies for Merck Research Laboratories. His research interests lie at the interface of organic and analytical chemistry, with particular emphasis on stereochemistry, separation science, and high-throughput analysis.

■ ACKNOWLEDGMENTS

We are grateful to the MRL New Technologies Review & Licensing Committee (NT-RLC) for providing funding for the instrumentation used in this study.

■ REFERENCES

(1) (a) Caron, S.; Dugger, R. W.; Ruggeri, S. G.; Ragan, J. A.; Brown Ripin, D. H. *Chem. Rev.* **2006**, *106*, 2943. (b) Goodman, S. N.; Dai, Q.; Wang, J.; Clark, W. M. *Org. Process Res. Dev.* **2011**, *15*, 123. (c) Steves, J. E.; Preger, Y.; Martinelli, J. R.; Welch, C. J.; Root, T. W.; Hawkins, J. M.; Stahl, S. S. *Org. Process Res. Dev.* **2015**, *19*, 1548.

(2) (a) Narayanam, J. M. R.; Stephenson, C. R. J. *Chem. Soc. Rev.* **2011**, *40*, 102. (b) Tucker, J. W.; Stephenson, C. R. J. *J. Org. Chem.* **2012**, *77*, 1617. (c) Prier, C. K.; Rankic, D. A.; MacMillan, D. W. C. *Chem. Rev.* **2013**, *113*, 5322.

(3) (a) Nicewicz, D. A.; MacMillan, D. W. C. *Science* **2008**, *322*, 77. (b) Ischay, M. A.; Anzovino, M. E.; Du, J.; Yoon, T. P. *J. Am. Chem. Soc.* **2008**, *130*, 12886. (c) Narayanam, J. M. R.; Tucker, J. W.; Stephenson, C. R. J. *J. Am. Chem. Soc.* **2009**, *131*, 8756.

(4) (a) Moeller, K. D. *Tetrahedron* **2000**, *56*, 9527. (b) Miller, A. K.; Hughes, C. C.; Kennedy-Smith, J. J.; Gradl, S. N.; Trauner, D. *J. Am. Chem. Soc.* **2006**, *128*, 17057. (c) Campbell, J. M.; Xu, H.-C.; Moeller, K. D. *J. Am. Chem. Soc.* **2012**, *134*, 18338. (d) Britton, W. E., Fry, A. J., Eds. *Topics in Organic Electrochemistry*; Springer, 2013. (e) O'Brien, A. G.; Maruyama, A.; Inokuma, Y.; Fujita, M.; Baran, P. S.; Blackmond, D. G. *Angew. Chem., Int. Ed.* **2014**, *53*, 11868.

(5) (a) Friedfeld, M. R.; Shevlin, M.; Hoyt, J. M.; Krska, S. W.; Tudge, M. T.; Chirik, P. J. *Science* **2013**, *342*, 1076. (b) Zuo, W.; Lough, A. J.; Li, Y. F.; Morris, R. H. *Science* **2013**, *342*, 1080. (c) Hoyt, J. M.; Schmidt, V. A.; Tondreau, A. M.; Chirik, P. J. *Science* **2015**, *349*, 960.

(6) (a) Plietker, B., Ed. *Iron Catalysis in Organic Chemistry: Reactions and Applications*;, Wiley−VCH, 2008. (b) Rodriguez-Ruiz, V.; Carlino, R.; Bezzenine-Lafollée, S.; Gil, R.; Prim, D.; Schulz, E.; Hannedouche, J. *Dalton Trans.* **2015**, *44*, 12029.

(7) Chirik, P. J.; Wieghardt, K. *Science* **2010**, *327*, 794.

(8) Zavoisky, E. *J. Phys. USSR* **1945**, *9*, 211.

(9) (a) Weil, J. A.; Bolton, J. R. *Electron Paramagnetic Resonance Spectroscopy: Elementary Theory and Applications*, 2nd ed.; Wiley-Interscience, 2007. (b) Brustolon, M., Giamello, E., Eds. *Electron Paramagnetic Resonance: A Practicioner's Toolkit*; Wiley-Interscience, 2009. (c) Drescher, M., Jeschke, G., Eds. *EPR Spectroscopy: Applications in Chemistry and Biology*; Springer-Verlag 2012.

DOI: 10.1021/acs.joc.6b00937
J. Org. Chem. 2016, 81, 6937−6944

(10) Carini, M.; Aldini, G.; Orioli, M.; Facino, R. M. *Curr. Pharm. Anal.* **2006**, *2*, 141.
(11) Kempe, S.; Metz, H.; Mäder, K. *Eur. J. Pharm. Biopharm.* **2010**, *74*, 55.
(12) For related examples, see: (a) Chappell, J.; Chiswell, B.; Canning, A. *Talanta* **1998**, *46*, 23. (b) Cordischi, D.; Occhiuzzi, M.; Dragone, R. *Appl. Magn. Reson.* **1999**, *16*, 427. (c) Yordanov, N. D.; Ranguelova, K. *Spectrochim. Acta, Part A* **2000**, *56*, 373.
(13) Pennington, J.; Cohen, R. D.; Tian, Y.; Boulineau, F. *J. Pharm. Biomed. Anal.* **2015**, *114*, 488.
(14) Liu, Y.; Mangion, I. Manuscript in preparation.
(15) For quantification of very low level of radicals dissolved in solvents of large electrical dipoles, a flat cell may be preferable as it allows for a much larger sample volume.
(16) (a) Su, Y.; Straathof, N. J. W.; Hessel, V.; Noel, T. *Chem. - Eur. J.* **2014**, *20*, 10562. (b) Yayla, H.; Peng, F.; Mangion, I. K.; McLaughlin, M.; Campeau, L.-C.; Davies, I.; DiRocco, D.; Knowles, R. R. *Chemical Science* **2016**, *7*, 2066.
(17) (a) Liu, J.; Liu, Q.; Yi, H.; Qin, C.; Bai, R.; Qi, X.; Lan, Y.; Lei, A. *Angew. Chem., Int. Ed.* **2014**, *53*, 502. (b) Ma, Y.; Yan, Z.; Bian, C.; Li, K.; Zhang, X.; Wang, M.; Gao, X.; Zhang, H.; Lei, A. *Chem. Commun.* **2015**, *51*, 10524.
(18) Nicewicz, D. A.; Nguyen, T. M. *ACS Catal.* **2014**, *4*, 355.
(19) EPR experiments performed in a frozen benzonitrile solution at 223 K. See also: Fukuzumi, S.; Kotani, H.; Ohkubo, K.; Ogo, S.; Tkachenko, N. V.; Lemmetyinen, H. *J. Am. Chem. Soc.* **2004**, *126*, 1600.
(20) For a related study, see: van Willigen, H.; Jones, G.; Farahat, M. S. *J. Phys. Chem.* **1996**, *100*, 3312.
(21) For detailed discussions of the excited state of compound **1**, see: (a) Benniston, A. C.; Harriman, A.; Li, P.; Rostron, J. P.; Verhoeven, J. W. *Chem. Commun.* **2005**, 2701. (b) Ohkubo, K.; Kotani, H.; Fukuzumi, S. *Chem. Commun.* **2005**, 4520. (c) Romero, N. A.; Nicewicz, D. A. *J. Am. Chem. Soc.* **2014**, *136*, 17024.
(22) Joshi-Pangu, A.; Lévesque, F.; Nicewicz, D.; DiRocco, D. Manuscript in preparation.
(23) (a) Shin-ya, K.; Furihata, K.; Teshima, Y.; Hayakawa, Y.; Seto, H. *Tetrahedron Lett.* **1992**, *33*, 7025. (b) Gould, S. J.; Melville, C. R. *Bioorg. Med. Chem. Lett.* **1995**, *5*, 51. (c) Gould, S. J.; Melville, C. R.; Cone, M. C.; Chen, J.; Carney, J. R. *J. Org. Chem.* **1997**, *62*, 320.
(24) (a) Fallis, I. A.; Murphy, D. M.; Willock, D. J.; Tucker, R. J.; Farley, R. D.; Jenkins, R.; Strevens, R. R. *J. Am. Chem. Soc.* **2004**, *126*, 15660. (b) Schley, N. D.; Fu, G. C. *J. Am. Chem. Soc.* **2014**, *136*, 16588. (c) Tarantino, K. T.; Miller, D. C.; Callon, T. A.; Knowles, R. R. *J. Am. Chem. Soc.* **2015**, *137*, 6440.
(25) Walker, F. A. *The Porphyrin Handbook*; Elsevier, 1999; Vol. 3, pp 81−183.
(26) EPR spectra of toluene solutions of **6** and **7** acquired at 298 and 90 K. A microwave power of 0.2 mW and a modulation field of 4 G at 100 kHz were employed for all measurements.
(27) (a) Janzen, E. G.; Blackburn, B. J. *J. Am. Chem. Soc.* **1968**, *90*, 5909. (b) Janzen, E. G.; Blackburn, B. J. *Acc. Chem. Res.* **1971**, *4*, 31.
(28) (a) Katritzky, A. R.; He, H.-Y.; Qiu, G.; Bratt, P. J.; Parrish, S. H., Jr.; Angerhofer, A. *Org. Lett.* **1999**, *1*, 1755. (b) Alberti, A.; Benaglia, M.; Macciantelli, D. *Org. Lett.* **2000**, *2*, 1553.
(29) (a) Perkins, M. J. *Adv. Phys. Chem.* **1980**, *17*, 1. (b) Tordo, P. In *Electron Spin Resonance. A Specialist Periodical Report*; Gilbert, B. C., Atherton, N. M., Davis, M. G., Eds.; The Royal Society of Chemistry: London, 1998; p 116. (c) Johnston, E. J.; Rylott, E. L.; Beynon, E.; Lorenz, A.; Chechik, V.; Bruce, N. C. *Science* **2015**, *349*, 1072.
(30) (a) Uchida, M.; Ono, M. *J. Am. Soc. Brew. Chem.* **1996**, *54*, 198. (b) Uchida, M.; Suga, S.; Ono, M. *J. Am. Soc. Brew. Chem.* **1996**, *54*, 205.
(31) (a) Andersen, M. L.; Skibsted, L. H. *J. Agric. Food Chem.* **1998**, *46*, 1272. (b) Andersen, M. L.; Outtrup, H.; Skibsted, L. H. *J. Agric. Food Chem.* **2000**, *48*, 3106.
(32) a^N = 15.3 G, a_β^N = 3.3 G for the first species and a^N = 16.4 G, a_β^N = 3.7 G for the second species.

DOI: 10.1021/acs.joc.6b00937
J. Org. Chem. 2016, 81, 6937−6944